Molecular Electronics

The Molecule–Electrode Interface in Single-Molecule Transistors**

*Hongbin Yu, Yi Luo, Kristen Beverly, J. Fraser Stoddart, Hsian-Rong Tseng, and James R. Heath**

A fundamental goal of molecular electronics[1] is to design useful transport signatures into solid-state devices through control[2] over the molecular components. In principle, theory and experiment should unite to provide a "chemical intuition" that guides 1) the direction of molecular design and synthesis and 2) the choice of the device materials and architectures that are employed in molecular electronics. To date, however, the field has advanced largely through the development of phenomenological—rather than quantitative—models of molecular devices. For example, traditional models for correlating properties, such as intermolecular charge transfer with molecular structure (electron-transfer theory) are designed for the solution phase.[3] Similarly, such structure–property relationships can be tested by using a variety of sophisticated spectroscopic techniques, such as optical measurements and multidimensional NMR spectroscopy, which have been designed to work in solution on statistical numbers of molecules.

Consider the case of a single molecule bridging two electrodes. Any theory of such a system must consider the molecule and the electrode as a single nonseparable entity.[4] The objectives of the theory would be 1) to predict the alignment of the Fermi levels of the electrodes with the molecular orbital energies in the molecule, 2) to forecast the voltage-dependent electron conductance across the molecule–electrode interfaces of the device junction, and 3) to provide fundamental insight that can be fed back into molecular and device design for optimization of properties. Ideal experiments should be able to provide a robust test of such predictions. This theory does not exist yet, and, until recently, there were very few experiments that could be used to guide or test such a theory. The situation is now changing, as increasingly reliable measurements of molecular electronic devices have been carried out in many laboratories.[5]

In particular, single-molecule devices are emerging as a powerful high-resolution spectroscopic tool for molecular electronics. Early experiments utilized[6] two-terminal break junctions in which one or a few molecules were suspended across a mechanically adjusted electrode gap. More recent experiments have employed[7–9] an electrical break junction, together with a gate electrode, to form a three-terminal device (3TD). The gate can be utilized to correlate the molecular energy levels with the Fermi energies of the electrodes, and thus somewhat normalize out the device-to-device fluctuations that are observed in the two-electrode measurements.

Herein we utilize single-molecule 3TDs with a Pt break-junction source and drain electrodes to investigate four molecules—namely, the bistable [2]rotaxane **AR**$^{4+}$ and **SR**$^{4+}$ and the corresponding dumbbell-shaped compounds **AD** and **SD**, from which the mechanically, redox-switchable rotaxanes were obtained (Scheme 1) by a template-directed protocol[10] that clips a tetracationic ring around the tetrathiafulvalene (TTF) units in the dumbbell-shaped compounds. Our goal was to address the nature of the molecule–electrode contact. We had previously found that similar amphiphilic, bistable [2]rotaxanes[11] and bistable [2]catenanes[12]—rendered amphiphilic with dimiristoylphosphatidic acid (DMPA) counterions—could be utilized[13,14] as solid-state, bistable switches in devices in which a Langmuir–Blodgett (LB) monolayer is sandwiched between a Si bottom electrode—passivated with the native oxide—and a Ti/Al top electrode. In the case of bistable [2]catenanes that were specially designed to interact noncovalently with the side walls of single-walled carbon nanotubes (SWNTs), we have also found[15] that usable switching devices could be fabricated using a semiconducting SWNT bottom electrode. Various control molecules, including the dumbbell precursors of the bistable [2]rotaxanes and nondegenerate [2]catenanes, were also explored, and none of these controls yielded a switch. Thus, we attributed the bistable character of working solid-state devices as arising from hysteretical mechanical motions in these redox-switchable interlocked molecules.[11,12] Conversely, we have never observed switching signatures attributable to a molecular bistability when we have utilized a metal (Au or Pt) bottom electrode.[16] One possible reason for the difference between Group IV (Si or C) electrode materials and transition metal electrodes is that the increased ionic character of the organic/metal interface leads to Schottky-like barriers to charge-flow, and that those barriers dominate the device characteristics. We report here that the device characteristics of 3TDs containing bistable [2]rotaxanes and Pt electrodes are extremely sensitive to the chemical nature of the molecule–-electrode contact, but are much less sensitive to the details of the molecular structure away from those contacts. This result has strong implications for the design of molecular electronic devices.

While the bistable [2]rotaxane **AR**$^{4+}$ can form "chemical" bonds between the terminal, incipient five-membered disulfide ring and a Pt electrode, the tetraarylmethane stopper at the other end of **AR**$^{4+}$ will, at most, become physisorbed onto platinum, thus the molecule–electrode contacts are asymmetric. In the case of the bistable [2]rotaxane **SR**$^{4+}$, both ends

---

[*] Prof. J. R. Heath, Dr. H. Yu, Dr. Y. Luo, K. Beverly
Caltech Chemistry, MC 127-72
1200 East California Boulevard, Pasadena, CA 91125 (USA)
Fax: (+1) 310-206-4038
E-mail: heath@caltech.edu
Prof. J. F. Stoddart, Dr. H.-R. Tseng
The California NanoSystems Institute and
Department of Chemistry and Biochemistry
University of California, Los Angeles
405 Hilgard Avenue, Los Angeles, CA 90095-1569 (USA)

[**] We thank Professor Hongkun Park and Wenjie Liang for helpful discussions, and the Department of Energy (DOE) and the Defense Advanced Research Projects Agency (DARPA), including the MARCO Center, for funding.

Supporting information for this article is available on the WWW under http://www.angewandte.org or from the author.

DOI: 10.1002/ange.200352352

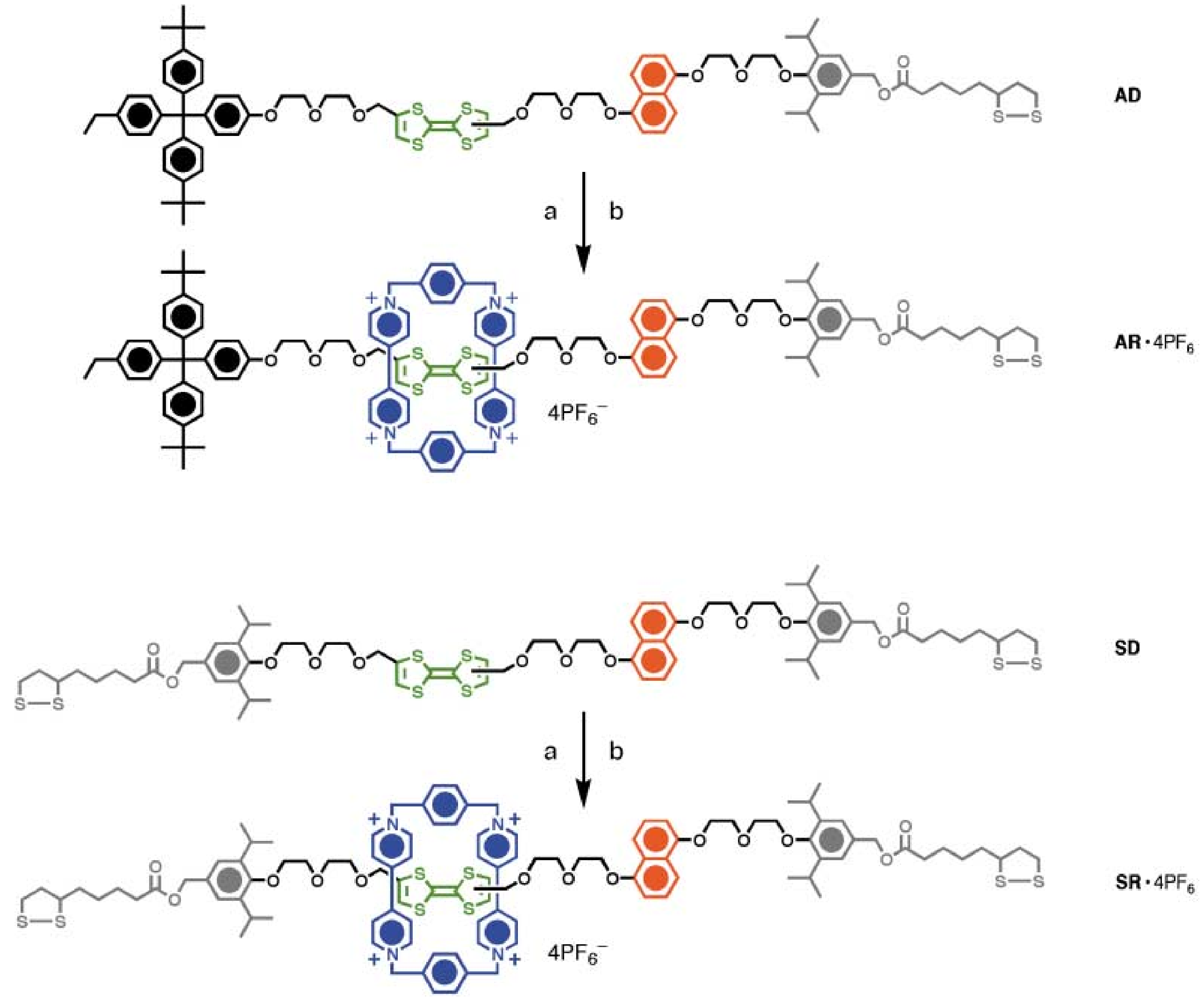

Scheme 1. Template-directed synthesis of **AR**·4 PF_6 from **AD**, and **SR**·4 PF_6 from **SD** in 77 and 34% yields, respectively. Reagents and conditions: a) α,α′-[1,4-phenylenebis(methylene)]bis(4,4′-bipyridium) bis(hexafluorophosphate), 1,4-bis(bromomethyl)benzene, DMF, RT, 10 days; b) chromatography on SiO_2 with Me_2CO/NH_4PF_6, followed by addition of H_2O to the eluent.

of the molecule are terminated by five-membered disulfide rings and so the molecule–electrode contacts are symmetric. It should be noted, however, that both molecules are asymmetric in their middle regions away from the contacts.

The devices used to conduct the single-molecule experiments are shown in Figure 1. A degeneratively doped (n^+)poly-Si substrate served as the gate electrode on top of which was grown a 30-nm thick SiO_2 film.[17] Each experimental run utilized 14 Pt junctions (thickness ca. 7 nm; width ca. 160 nm; length ca. 500 nm). These junctions were patterned by electron-beam lithography into a poly(methyl methacrylate) (PMMA) resist on top of the SiO_2 layer, and then developed by electron beam evaporation of Pt from a metal target. The patterns were cleaned with Me_2CO and an O_2 plasma, and then a drop of a dilute solution (ca. 10^{-6} M to 10^{-7} M) of the molecules of interest in CH_2Cl_2 was placed onto the device. These devices were dried under flowing N_2. The individual junctions were then wire-bonded, mounted into a chip carrier, and then loaded into the cold-finger of a He cryostat, which was cooled to 1.7 K. The junctions were broken by applying a voltage to the wire, as has been described by other research groups.[8,9] After forming the break junction, current–voltage (I–V) curves were measured across the source and drain electrodes as a function of varying gate voltage (V_G). Since the object was to prepare junctions containing just one molecule, most junctions were simply open circuits, which implies that no molecule was bridging the gap. For the device prepared with $\mathbf{AR}^{4+}$, 5 out of 40 broken junctions exhibited a gating response while, for $\mathbf{SR}^{4+}$ 7 out of 25 broken junctions exhibited a gating response. This higher yield for $\mathbf{SR}^{4+}$—which is chemisorbed to both the source and drain sides of the junction—was observed, even though the solution of $\mathbf{SR}^{4+}$ was a factor of four more dilute than for $\mathbf{AR}^{4+}$. Several break junctions were investigated by electron microscopy after completing the I–V measurements, and the gap was observed to be about 4 nm. Although this distance is hard to quantify, the result is consistent with a nonmeasurable tunneling current between the two electrodes in the absence

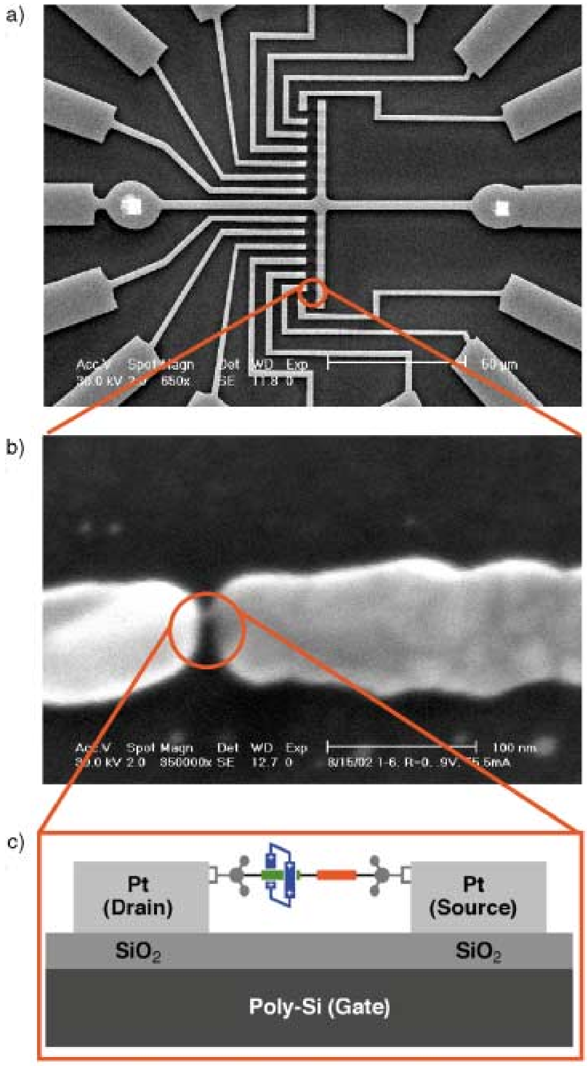

Figure 1. a) Scanning electron microscope (SEM) pictures of single-molecule devices fabricated on a Si substrate. A 30-nm thick low-temperature thermal oxide of Si was grown on top of a degenerately doped Si substrate. The center metal electrode, where the break junction is made of 7-nm thick Pt, followed by 100-nm thick gold wires and pads for wire bonding. b) The SEM image after the break junction is made. The separation between the two metal electrodes is around 4 nm. c) A section through a single-molecule transistor.

of a molecule. Tunneling current can be used to estimate the width of gaps in the 1–2-nm range.[7]

Figure 2 a,b display data from break junctions formed in the presence of **AR**$^{4+}$ and **SR**$^{4+}$. Here, the x-axis is the applied source-drain voltage (V_{SD}), and the y-axis is V_G.[18] The color represents the conductance (dI/dV) of the junction, which is typically ≥ 0 for all V_{SD} values. The darkest areas in the center of the plots indicate the regions of no current. The edges of these dark regions correspond to the current steps in the I–V graph near the threshold voltage. This behavior is that of a single-electron transistor—that is, a device containing a small island (the molecule) connected to electrodes by tunnel barriers at either end and with gate-voltage-tunable electronic states.[19] At low V_{SD} values, the electron energy is not high enough to tunnel to the island and, therefore, current is blocked (Coulomb blockade).[14] When voltage passes beyond the threshold, the electron gains sufficient energy and can tunnel to an electronic state on the molecule.

Although amphiphilic, bistable [2]rotaxanes that are structurally similar to **AR**$^{4+}$ and **SR**$^{4+}$ have been shown to work as solid-state switches in two-terminal tunnel junctions, such switching behavior is thermally activated.[14] The data displayed in Figure 2 was collected at 1.7 K, and so we expect that all activated processes will be quenched. With this type of measurement, it is never completely clear whether each device contains just one molecule, although each individual triangular-shaped resonance undoubtedly originates from a single molecule because of the extreme unlikelihood of having any two molecules coupled in the same way to the source, drain, and gate electrodes. In each plot, a region where the conductance gap narrows has been chosen (indicated by the red arrows). In Figure 2 c,d, the current–voltage response that correlates with the V_G values is presented, indicated by the arrows located at the sides of Figure 2 a,b, respectively.

Two significant results are illustrated in Figure 2. First, the conductance spectrum for **AR**$^{4+}$ is quite asymmetric, while the corresponding spectrum for **SR**$^{4+}$ is symmetric. This result was found for all of the devices measured. We may clearly ascribe it to the asymmetric/symmetric nature of the molecule–electrode chemical interactions. Both molecules are asymmetric structures, although only **SR**$^{4+}$ can have similar bonding at both the source and drain electrodes. Second, the junction resistance, measured at the point where the conductance gap narrows, is approximately a factor of 10^2 lower for **SR**$^{4+}$ than for **AR**$^{4+}$. Again, this result was observed in every device that was measured, and implies that this reduced junction resistance is attributable to the additional "chemical" bonding interaction possible for **SR**$^{4+}$. A third observation (Figure 3) was that, for junctions prepared using the dumbbell-shaped compounds **AD** and **SD**, the first two observations remained valid, namely, the conductance spectra (Figure 3 a,b) for **AD** and **SD** are asymmetric and symmetric, respectively. In Figure 3 c,d, the current–voltage response that correlates with a V_G-tuned closing of the conductance gap are presented, indicated by the arrows located at the sides of Figure 3 a,b, respectively. In other words, while changing the chemical nature of the molecule–electrode contacts has a profound effect on the conductance characteristics of the junction, changing the nature of the molecule away from those contacts had only a minor effect. A last relevant observation (not shown) involves the temperature-dependent stability of these devices. For devices containing **AR**$^{4+}$, the current decreased to below our detection limit of about 10^{-12} A when the temperature was raised to about 20 K. This result indicates that the molecule moved so that it was no longer bridging the source and drain electrodes. For **SR**$^{4+}$, conductance plots such as that presented in Figure 2 b could still be recorded when the temperature was raised to above 100 K, albeit with thermally broadened line widths, but also with increased current magnitudes. This observation is consistent with the fact that **AR**$^{4+}$ is chemisorbed to just one electrode and is loosely anchored (physisorbed) onto the other, while **SR**$^{4+}$ is chemisorbed to both electrodes.

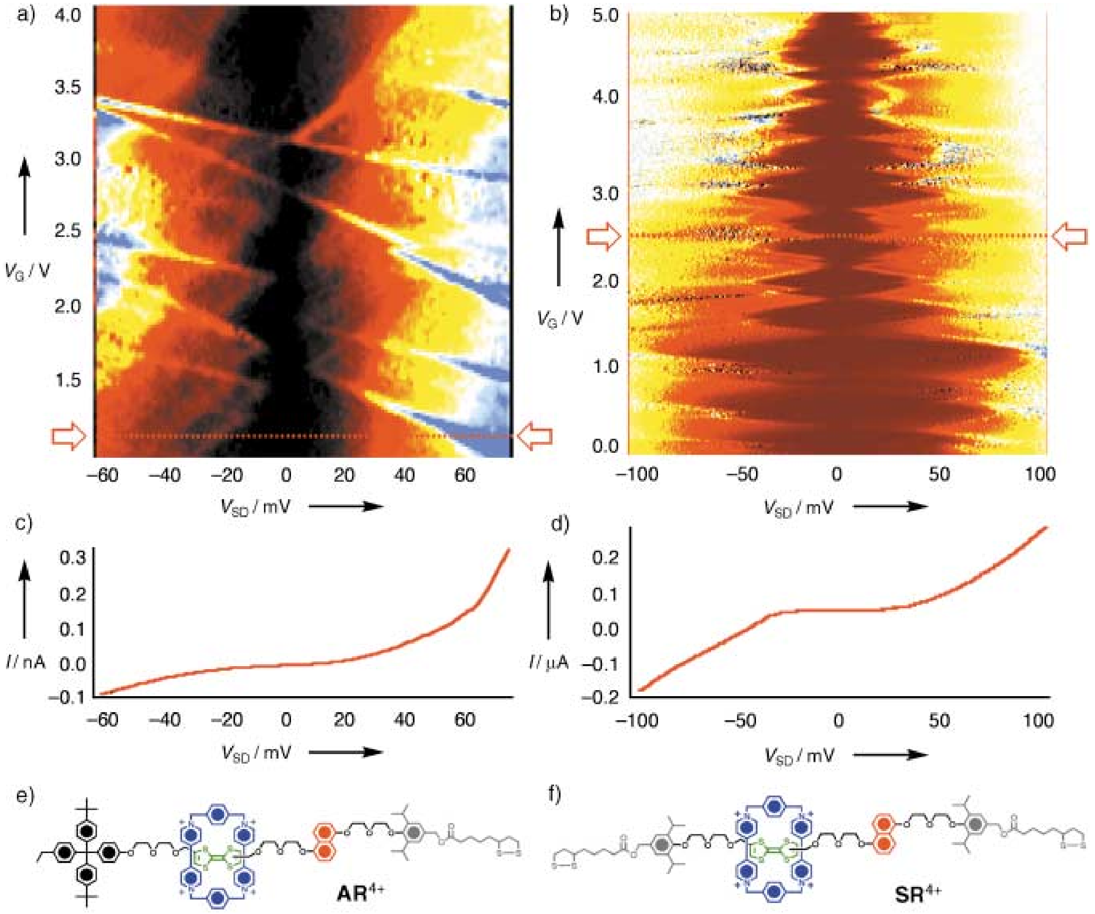

Figure 2. Differential conductance (dI/dV) plots (a and b) and current–voltage (I–V) curves (c and d) for rotaxane **AR**$^{4+}$ and **SR**$^{4+}$ (e and f). The I–V curves shown in (c) and (d) were taken at the gate voltages (V_G) indicated by the red arrows in (a) and (b), respectively.

The conclusion from all of these results taken together is that it is very easy to identify the molecular components involved in the molecule–electrode contacts in a system consisting of Pt electrodes and a molecule containing a large number of low-lying molecular orbitals. However, those same interface states also dominate the transport characteristics. The molecular orbitals that are not involved in the electrode contacts are effectively masked. Even something as simple as molecular asymmetry is difficult to detect.

These results, coupled with other results[13–15] using Si and SWNT electrodes, outline a significant chemical challenge for molecular electronics. If the goal of achieving interesting device signatures that are molecular in origin is achieved, then the implication is that such devices might be scalable to the dimensions of just a few molecules. However, at such small dimensions, the choice of conductors is limited. SWNTs are both "good molecular electronics electrodes" and good conductors, but, in spite of recent progress, sorting SWNTs by electrical character is still a significant challenge, and organizing SWNTs into well-defined circuit architectures is also nontrivial.[20,21] Ultra-high density circuits[22] of metal and semiconductor nanowires can be patterned with wire diameters of only a few nanometers, but at wire diameters below a few nanometers, only the metal wires are expected to be good conductors. Thus, the challenge is to design *chemically* a molecule–metal electrode interface that does not mask the electronic structure of the molecule. Yaliraki et al.[4a] have calculated that simply varying the electrode-binding atom on the organic molecule from O to S to Se for an Au electrode has a strong impact on the resulting transport characteristics through the molecular junction. Similarly, the exploration of other metals and metal alloys as electrode materials is likely to be fruitful. Theoretical guidance in such an exploration would be extremely helpful.

Received: July 10, 2003 [Z52352]

Keywords: break junctions · differential conductance · molecular devices · molecule electrode contact · rotaxanes

---

[1] A. Aviram, M. A. Ratner, *Chem. Phys. Lett.* **1974**, *29*, 277–283.
[2] J. R. Heath, M. A. Ratner, *Phys. Today* **2003**, *56*, 43–49.
[3] J. Jortner, M. Bixon, A. A. Voityuk, N. Rösch, *J. Phys. Chem. A* **2002**, *106*, 7599–7606.
[4] a) S. N. Yaliraki, M. Kemp, M. A. Ratner, *J. Am. Chem. Soc.* **1999**, *121*, 3428–3434; b) K. W. Hipps, *Science* **2001**, *294*, 536–537; c) X. D. Cui, A. Primak, X. Zarate, J. Tomfohr, O. F. Sankey, A. L. Moore, T. A. Moore, D. Gust, G. Harris, S. M. Lindsay, *Science* **2001**, *294*, 571–574.

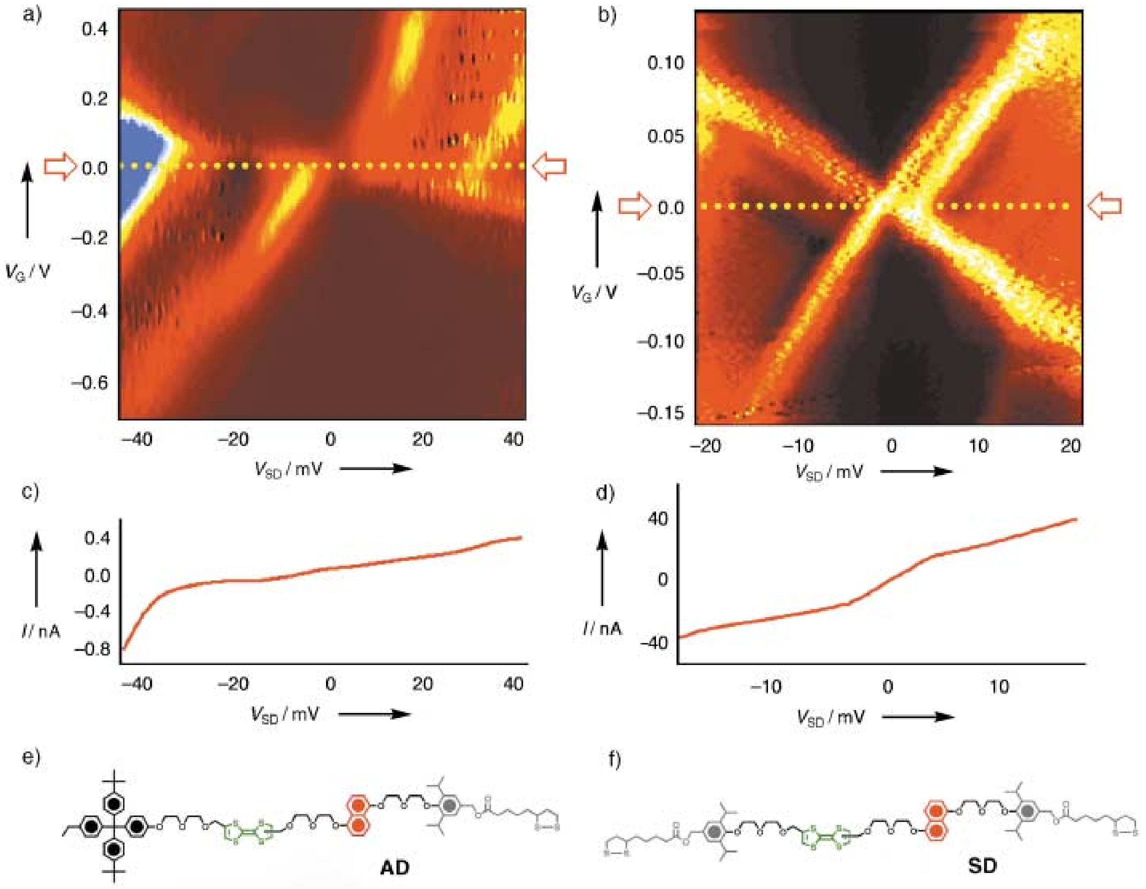

Figure 3. Differential conductance (d*I*/d*V*) plots (a and b) and current–voltage (*I*–*V*) curves (c and d) for the dumbbell-shaped compounds **AD** and **SD** (e and f). Note that, in concert with the data for the [2]rotaxanes, the chemical nature of the molecule–electrode contacts dominate both the magnitude of the current and the symmetry of the conductance plots. These high-resolution scans reveal the type of excited-state structure that is observed in simpler molecules. While the fine structure is relatively symmetric about $V_{SD}=0$, the current magnitude is not. The conductance plots are normalized such that the value of V_G, for which the conductance gap closes, is set to 0.

[5] a) D. Goldhaber-Gordon, M. S. Montemerlo, J. C. Love, G. J. Opiteck, *Proc. IEEE.* **1997**, *85*, 521–540; b) C. Joachim, J. K. Gimzewski, A. Aviram, *Nature* **2000**, *408*, 541–548; c) R. L. Carroll, C. B. Gorman, *Angew. Chem.* **2002**, *114*, 4556–4579; *Angew. Chem. Int. Ed.* **2002**, *41*, 4378–4400; d) M. Mayor, H. B. Weber, R. Waser in *Nanoelectronics and Information Technology. Advanced Electronic Materials and Novel Devices* (Ed.: R. Waser), Wiley-VCH, Weinheim, **2003**, pp. 501–525.

[6] M. A. Reed, C. Zhou, C. T. Muller, T. P. Burgin, J. M. Tour, *Science* **1997**, *278*, 252–254.

[7] H. Park, J. Park, A. K. L. Lim, E. H. Anderson, A. P. Alivisatos, P. L. McEuen, *Nature* **2000**, *407*, 57–60.

[8] J. Park, A. N. Pasupathy, J. I. Goldsmith, C. Chang, Y. Yaish, J. R. Petta, M. Rinkoski, J. P. Sethna, H. D. Abruña, P. L. McEuen, D. C. Ralph, *Nature* **2002**, *417*, 722–725.

[9] W. Liang, M. P. Shores, M. Bockrath, J. R. Long, H. Park, *Nature* **2002**, *417*, 725–729.

[10] J. F. Stoddart, H.-R. Tseng, *Proc. Natl. Acad. Sci. USA* **2002**, *99*, 4797–4800.

[11] a) J. O. Jeppesen, J. Perkins, J. Becher, J. F. Stoddart, *Org. Lett.* **2000**, *2*, 3547–3550; b) H.-R Tseng, S. A. Vignon, J. F. Stoddart, *Angew. Chem.* **2003**, *115*, 1529–1533; *Angew. Chem. Int. Ed.* **2003**, *42*, 1491–1495; c) J. O. Jeppesen, K. A. Nielsen, J. Perkins, S. A. Vignon, A. Di Fabio, R. Ballardini, M. T. Gandolfi, M. Venturi, V. Balzani, J. Becher, J. F. Stoddart, *Chem. Eur. J.* **2003**, *9*, 2982–3007.

[12] V. Balzani, A. Credi, G. Mattersteig, O. A. Matthews, F. M. Raymo, J. F. Stoddart, M. Venturi, A. J. P. White, D. J. Williams, *J. Org. Chem.* **2000**, *65*, 1924–1936.

[13] C. P. Collier, G. Mattersteig, E. W. Wong, Y. Luo, K. Beverly, J. Sampaio, F. M. Raymo, J. F. Stoddart, J. R. Heath, *Science* **2000**, *289*, 1172–1175.

[14] Y. Luo, C. P. Collier, J. O. Jeppesen, K. A. Nielsen, E. DeIonno, G. Ho, J. Perkins, H.-R. Tseng, T. Yamamoto, J. F. Stoddart, J. R. Heath, *ChemPhysChem* **2002**, *3*, 519–525.

[15] M. Diehl, D. W. Steuerman, H.-R. Tseng, S. A. Vignon, A. Star, P. C. Celestre, J. F. Stoddart, J. R. Heath, *ChemPhysChem* **2003**, *4*, in press.

[16] Other researchers have described bistability in junctions sandwiching a molecular monolayer between a metal bottom electrode and a Ti/Al top electrode. This bistability, however, is not dependent upon the details of the molecular material, and exhibits a very different electrical signature of the switching. For example, it is not thermally activated; see a) Y. Chen, D. A. A. Ohlberg, X. Li, D. R. Stewart, R. S. Williams, J. O. Jeppesen, K. A. Nielsen, J. F. Stoddart, D. L. Olynick, E. Anderson, *Appl. Phys. Lett.* **2003**, *82*, 1610–1612; b) Y. Chen, G.-Y. Jung, D. A. A. Ohlberg, X. Li, D. R. Stewart, J. O. Jeppesen, K. A. Nielsen, J. F. Stoddart, R. S. Williams, *Nanotechnology* **2003**, *14*, 462–468.

[17] The 30-nm thick SiO_2 gate insulator was grown at 450 °C using low-pressure chemical vapor deposition. Leakage currents between the gate and the source or drain electrodes were less than 10^{-12} A for gate voltages up to 35 V.

[18] We note that the gate coupling to the molecules is strong in our devices. From the slope of the differential conductance plot, we can estimate that a change of about 300 mV in the gate-voltage translates into a change of about 100 mV in the source-drain bias. This coupling strength is significantly greater than any previously reported, and allows us to access a larger range of the molecular electronic energy levels by varying the gate bias. This increased coupling strength is probably attributable to the use of Pt break junctions, which allows for the fabrication of much thinner electrodes.

[19] H. Grabert, M. H. Devoret, *Single Charge Tunneling*, Plenum, New York, **1992**.

[20] D. Chattopadhyay, I. Galeska, F. Papadimitrakopoulos, *J. Am. Chem. Soc.* **2003**, *125*, 3370 – 3375.

[21] R. Krupke, F. Hennrich, H. v. Löhneysen, M. M. Kappes, *Science*, **2003**, *301*, 344 – 347.

[22] N. Melosh, A. Boukai, F. Diana, B. Geradot, A. Badolato, P. Petroff, J. R. Heath, *Science* **2003**, *300*, 112 – 114.